Marine Pollution Bulletin 182 (2022) 113976

Contents lists available at ScienceDirect

Marine Pollution Bulletin

journal homepage: www.elsevier.com/locate/marpolbul

Observational and model studies on transport and inventory of microplastics from a leak accident on the beaches of Yantai

Chen Zhang [a], Qing Wang [b,*], Jianmin Zhao [a,b,c], Yingjie Zhao [d], Encui Shan [b]

[a] Muping Coastal Environment Research Station, Yantai Institute of Coastal Zone Research, Chinese Academy of Sciences, Yantai 264003, PR China
[b] Research and Development Center for Efficient Utilization of Coastal Bioresources, Yantai Institute of Coastal Zone Research, Chinese Academy of Sciences, Yantai 264003, PR China
[c] Center for Ocean Mega-Science, Chinese Academy of Sciences, Qingdao 266071, PR China
[d] Harbin Institute of Technology, School of Marine Science and Technology, Weihai 264209, PR China

ARTICLE INFO

Keywords:
Microplastics
Lagrangian TRANSport model
Beach sediments
Microplastic leakage accident
Bohai Sea

ABSTRACT

We investigated an unexpected microplastic (MP) leakage event that occurred along the coastline of Yantai in January 2021. Sediment samples were collected from three zones on 9 beaches. MPs were identified with an average abundance of 247.6 ± 125.6 items/m^2 on 7 beaches. The total amount of MPs from the leak accident was estimated to be 1.50×10^7 items (514.67 kg). The MPs were identified as polyethylene (PE), polypropylene (PP), and PP/PE blends using μ-FT-IR analysis. By utilizing a numerical model, the transmission process and potential source of MPs were demonstrated. The modeling results showed that the MPs might originate from the central and western part of the Bohai Sea and be driven to the beaches of Yantai by northwest wind and wind-induced surface current. However, due to the absence of direct evidence, the simulation results might only indicate the range of the leaking source, which was the movement trajectory of MPs.

1. Introduction

Over 300 million tons of plastic products were manufactured worldwide, and about 8 million tons were discharged into the ocean each year (Plastics Europe, 2018; Jambeck et al., 2015; Eriksen et al., 2014; Rochman, 2018). Meanwhile, microplastic particles (<5 mm in diameter) as a direct or indirect production from plastic industry are widely detected in various marine habitats, including water, sediments, and even polar region (Li et al., 2020; Su et al., 2022; Constant et al., 2020; Pohl et al., 2020). Due to the potential risk of MPs to marine ecosystems, governments and scholars have aroused great concern about the distribution and inventory of MPs in the marine environment and the influence on aquatic organisms (Thompson et al., 2004; Peng et al., 2020; Wang et al., 2019; Teng et al., 2021).

Since the coastal areas were both a vital sink and transmission channel of MPs, growing attention has been drawn to the occurrence of coastal MPs pollution (Bridson et al., 2020; Maynard et al., 2021; Zhang et al., 2020). The contaminated beaches suffered from not only terrestrial pollution but also water-borne transportation pollution. Previous studies have confirmed the sources, sinks, and pathways of MPs in some sea areas. However, a complete description of MPs immigration in the marine environment remains unclear (Jiang et al., 2020; Su et al., 2022).

Since understanding the movement and accumulation of MPs enables an evaluation of ecological impacts, numerical models are widely used to comprehend the transport of MPs under the hydrodynamic force (Frère et al., 2017; Hardesty et al., 2017; Genc et al., 2020; Besseling et al., 2016). Modeling results show that under the influence of current and wind, the plastic debris can be transmitted over a long distance, reach and accumulate at the coastlines far from its source (Jiang et al., 2020; Liubartseva et al., 2016; Sherman and van Sebille, 2016).

The Bohai Sea is the largest inner sea of China, with a total coastal population of >70 million. It was surrounded by three inner bays on three sides: Bohai Bay (BHB) in the west, Liaodong Bay (LDB) in the north and Laizhou Bay (LZB) in the south. The Bohai Strait was the only passage for the exchange of material and water between the Bohai Sea and the Yellow Sea (Ding et al., 2019). Adjacent to the southern end of the Bohai Strait, Yantai is an important tourist and port city in northern China, with a coastline of 702.5 km and a population of 7.1 million. With the rapid economic growth and deterioration of the water quality of the Bohai Sea, the coastal environment around Yantai is under tremendous pressure (Zhang et al., 2019).

In mid-January 2021, a large number of plastic particles (raw

* Corresponding author.
E-mail address: qingwang@yic.ac.cn (Q. Wang).

https://doi.org/10.1016/j.marpolbul.2022.113976
Received 24 May 2022; Received in revised form 20 July 2022; Accepted 21 July 2022
Available online 31 July 2022

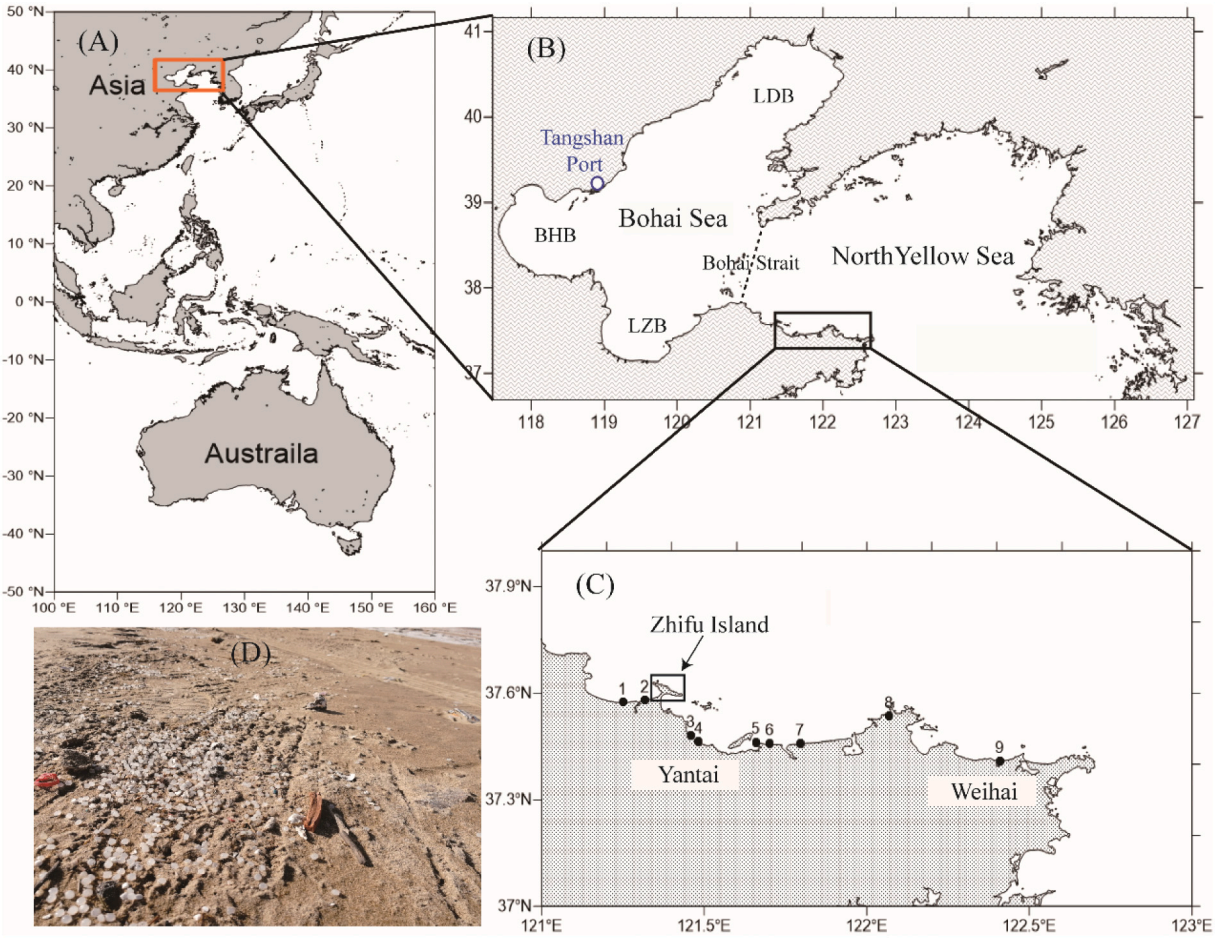

Fig. 1. Map containing simulation area (the orange rectangle) and sampling area (the black rectangle) (A), the numerical simulation area (B), sampling sites (C), and an image of a sampling beach (D).

materials, sizes <5 mm) suddenly appeared on the beaches along the coastline of Yantai (https://xhpfmapi.zhongguowangshi.com/vh512/handshoot/detail/296001). A survey along the coastline was conducted, and the sediment samples from contaminated areas were collected and analyzed. Based on the sampling data, the scope and extent of plastic pollution were investigated, and numerical simulation experiments were conducted to reveal the possible source and pathway of these pollutants. This work also emphasizes the effects of wind drag on the transmission of sea surface MPs.

2. Materials and methods

2.1. Study area

In order to determine the extent and the abundance of MPs, sediments were collected from nine beaches along the coast of Yantai and its neighboring city (Weihai) during January 17–18, 2021. The numerical model was used to trace the source and the pathway of these contaminants. The sampling stations are Yantai golden beach (S1), Lubao beach (S2), Yantai university beach (S3), Tianyue bay beach (S4), Libeng island beach (S5), Muping beach (S6), Dongfang sea beach (S7), Weihai golden beach (S8), Naxiang sea beach (S9) from west to east successively, which are located between 37.41° and 37.58° north latitude and 121.25° to 122.41° east longitude (Fig. 1). The sites S1-S7 are along the coast of Yantai, while S8 and S9 are located in Weihai, a tourist and port city. The detailed information on sampling sites is provided in Table S1.

2.2. Sample collection and analysis

A modified method was used to collect the sediment samples on the beach (Lee et al., 2017; Maynard et al., 2021; Piñon-Colin et al., 2018). Three 100-m-long sampling lines in backshore (BS), high tide line (HT), and low tide line (LT) areas were placed on each beach. During the sampling, we found that no MPs from this leakage accident were below the depth of 2.5 cm. Thus, along each sampling line, five 50 cm (length) × 50 cm (width) × 2.5 cm (depth) quadrats were randomly selected with at least 20-m interval (Lee et al., 2017). Sediment samples of each quadrat were placed into aluminum foil bags with a metal shovel (Qiu et al., 2016).

After being transported to the laboratory, the sediment samples were dried at 60 °C for 48 h, and the sediment samples were sieved with a 1-mm mesh sieve (Gao et al., 2021). The MPs appeared in this event were easily identified with a size of >2 mm, a shape of the approximate ellipsoid, and non-transparent milky white. Therefore, all particles with obviously different appearances were eliminated. Before further examination, the particulates were oxidized using 30 % H_2O_2 for 24 h to digest biogenic materials (Teng et al., 2020) and washed with Milli-Q water. After dried at 60 °C, all the MPs were weighed and characterized by shapes. The images of MPs were taken by the stereomicroscope (Olympus, SZX10, Japan) equipped with a camera (CnoptecTP510, Chongqing, China), and the length of individual MPs were measured by using an image processing software. The Qa/Qc of this analysis was supplied in supporting information.

Fourier transform infrared microspectroscopy (μ-FT-IR) was applied to identify the polymer composition of the MPs. A number of 100 MPs

Table 1
The abundance and morphological characteristics of MPs in beach sediments collected from different sites.

	S1 HT	S2 HT	S2 BS	S4 TH	S5 HT	S6 HT	S7 HT	S8 HT	S8 BS
Abundance of ellipsoidal MPs (items/m^2)	840.8 ± 512.2	1476.0 ± 644.4	52.2 ± 52.0	88.6 ± 40.2	260.6 ± 128.8	172.8 ± 124.6	96.4 ± 64.4	304.4 ± 96.6	16.2 ± 4.8
Abundance of columnar MPs (items/m^2)	8.2 ± 8.0	112.8 ± 48.8	4.0 ± 4.3	0	20.8 ± 12.2	12.4 ± 12.6	8.6 ± 4.6	4.2 ± 4.4	0
Diameter of ellipsoidal MPs (2R) (cm)	4.25 ± 0.28	4.21 ± 0.28	4.28 ± 0.24	4.24 ± 0.26	4.23 ± 0.32	4.23 ± 0.29	4.30 ± 0.34	4.21 ± 0.30	3.98 ± 0.31
Diameter of ellipsoidal MPs (2r) (cm)	3.84 ± 0.27	3.88 ± 0.27	3.91 ± 0.21	3.82 ± 0.26	3.90 ± 0.26	3.91 ± 0.26	3.90 ± 0.23	3.78 ± 0.26	3.49 ± 0.34
Major axis of columnar MPs (L) (cm)	3.59 ± 0.31	3.29 ± 0.29	3.25 ± 0.05	–	3.65 ± 0.25	3.69 ± 0.19	3.73 ± 0.32	3.78 ± 0.31	–
Minor axis of columnar MPs (d) (cm)	2.86 ± 0.23	2.98 ± 0.23	3.20 ± 0.12	–	2.80 ± 0.21	2.81 ± 0.26	2.76 ± 0.08	2.75 ± 0.36	–
Height of columnar MPs (h) (cm)	3.18 ± 0.06	3.23 ± 0.10	3.21 ± 0.04	–	3.10 ± 0.05	3.19 ± 0.08	3.12 ± 0.15	3.20 ± 0.09	–

particles (accounting for about 2.3 % total samples) were randomly selected from all the sampling sites and placed on the ultra-fast motorized stage of a Nicolet™ iN10 infrared microscope (Thermo Fisher Scientific, USA) and measured in the transmittance mode by the MCT detector. The detector spectrum was 650–4000 cm^{-1}, co-adding 128 scans at a resolution of 8 cm^{-1}. The aperture was set at 150 × 150 μm. The spectra were obtained with the OMNIC software (Thermo Scientific, Madison, USA) and compared with the OMNIC polymer spectra library. Only when the match was >70 %, the particle can be considered as MPs (Zhao et al., 2018).

Analysis of variance (ANOVA) and nonparametric test of Kruskal-Wallis test with post hoc tests were performed on the difference of MPs abundance among different sampling sites. All results were considered statistically significant at $P < 0.05$. The statistical analyses were performed using SAS (version 9.2) and Excel 2013 software. The abundance of MPs was calculated by the MPs number by the sample area (0.5 × 0.5 m^2) and expressed as the MPs number per square meter. MP's abundance, size, and mass are given as mean ± SD. The plots were drawn through ArcGIS 10.0 and Matlab 2015.

2.3. MPs quantification

The volume, the mass, and the number of MPs leaked in this incident were calculated in the following form:

$$\overline{V_E} = 4/3{*}\pi{*}\overline{r^2}{*}\overline{R} \tag{2-1}$$

$$\overline{V_C} = \pi{*}\overline{L}{*}\overline{d}{*}\overline{h} \tag{2-2}$$

$$\overline{V_A} = \overline{V_E}{*}N_E + \overline{V_C}{*}N_C \tag{2-3}$$

$$\overline{M_A} = \overline{M_E}{*}N_E + \overline{M_C}{*}N_C \tag{2-4}$$

$$V_T = \sum_{m=1}^{n} X_m{*}\overline{V_A} \tag{2-5}$$

$$M_T = \sum_{m=1}^{n} X_m{*}\overline{M_A} \tag{2-6}$$

$$N_T = \sum_{m=1}^{n} X_m{*}\overline{N_A} \tag{2-7}$$

In Eqs. (2-1) to (2-7), $\overline{V_E}$ and $\overline{V_C}$ are the average volume of the individual ellipsoidal and columnar MPs. $\overline{R}$ and $\overline{r}$ are the two radii of ellipsoid. $\overline{L}$ and $\overline{d}$ are the major and minor axis of columnar MPs. $\overline{h}$ is the height of the column. $\overline{V_A}$ and $\overline{M_A}$ are average volume and mass of a square meter of sampling beach. $\overline{M_E}$ and $\overline{M_C}$ are the average mass of individual ellipsoidal and columnar MPs. V_T, M_T and N_T are the total volume, mass and number of MPs on the beaches of Yantai. X_m is the length along the coastline in each site, which is exacted from the software of Google Earth. n stands for the number of the sampling sites. The particle-size information ($\overline{R}$, $\overline{r}$, $\overline{L}$, $\overline{d}$ and $\overline{h}$) used to calculate the volume ($\overline{V_E}$ and $\overline{V_C}$) were the average values of all samples in each site and listed in Table 1.

2.4. Ocean dynamic model

In this study, we coupled the Lagrangian TRANSport model (LTRANS) and ocean dynamic model to simulate the MPs transport in the Bohai Sea. The Regional Ocean Modeling System (ROMS, UCLA version) was used to simulate the dynamic environment in Bohai Sea from November 15, 2020 to January 16, 2021. ROMS is a three dimension (3-D), free surface, terrain-following, hydrodynamic model and can provide 3-D current to LTRANS. It successfully simulated the dynamic environment of the Bohai Sea (Mo et al., 2016; Li et al., 2018). Further explanation of ROMS can be found in the research (Shchepetkin and McWilliams, 2005). A 2 × 2 km horizontal resolution and 20 vertical layers with a minimum depth of 0.1 m were adopted here. The boundary and initial fields were obtained from data-assimilative hybrid isopycnal-sigma-pressure coordinate ocean model (HYCOM, GLBa0.08/expt_90.6). The wind data from European Center for Medium-Range Weather Forecasts (ECMWF) were used to drive ROMS and to investigate the wind drag on MPs of the sea surface. Through calculating wind-induced current in ROMS and adding wind drag components to LTRANS, we added the influence of wind on MPs to simulate the results (Alosairi et al., 2020; Tsiaras et al., 2021). Tidal data were derived from the tidal database of the Advanced Circulation Model with nine tidal constituents (K1, O1, Q1, M2, S2, N2, K2, M4, and M6). The outputs of ROMS, including current, temperature, and salinity, were provided to LTRANS as forcing fields with 1-hour temporal resolution.

2.5. Lagrangian TRANSport model

LTRANS were used to simulate the transport of leaked MPs in this event. LTRANS was widely used in predicting the movement of passive particles (Goodwin et al., 2019; North et al., 2008; Zhang et al., 2016) with a random displacement module for turbulent motion, a 4th order Runge-Kutta advection scheme, and a sinking/floating module for particles. In this study, the spatial resolution of LTRANS was set to the same as ROMS. All water properties were interpolated from the ROMS grid and time step to LTRANS (Brickman and Smith, 2002; Li et al., 2005; Neumann et al., 2014). The relevant information of LTRANS was

Table 2
The abundances of MPs on different beach sediments around the world.

Region	Abundance (items/m^2)	Reference
Yantai, China	247.6 ± 125.6	This study
Dubai, UAE	165	Aslam et al., 2020
Taiwan, China	529	Kunz et al., 2016
Tenerife, Spain	532.8	Alvarez-Hernandez et al., 2019
Qingdao, China	119.44 ± 30.78	Gao et al., 2021
Auckland, New Zealand	459	Bridson et al., 2020
Ross Sea, Antarctica	1.15–168.4	Munari et al., 2017
South Carolina, United States	413.8 ± 76.7 and 221.0 ± 25.6	Gray et al., 2018
South Korea	897.3	Lee et al., 2015
Brazil	30.4 and 17.4	Maynard et al., 2021

supplied in supporting information, and the complete description can be found in North et al. (2008). The input sources of MPs in LTRANS were selected from the sampling sites where MPs were detected, and in each site, 400 MPs particles were released on January 16, 2021. Two backward simulation experiments were performed to reveal the trajectory of MPs and trace back to the possible sources from November 17, 2020, to January 16, 2021. One (Scenario 1) was conducted under the influence of wind drag on sea surface particles, and the other (Scenario 2) was not. The directions of the wind and current input into the backward simulations have the same value but contrary signs and chronological order with the ECMWF data and the output of ROMS. Compared with the actual situation, the particles in the backward simulation move along the same trajectory in the opposite direction. Since the MPs in this event were diagnosed as low-density particles (<sea water), all the particles were regarded as floating objects in simulation experiments.

3. Results and discussion

3.1. Abundance of MPs

The sampling results showed that the microplastic leakage pollution event affected most beach areas of Yantai. MPs were detected in all sites besides S3 and S9 (Fig. 3). Since our study was to confirm the contamination range and degree of MPs in the affected areas, all non-contaminated sites (S3 and S9) were excluded from the statistics of MPs abundance. The total number of MPs in sampled sediments was 4333 items. Furthermore, 97.9 % of MPs were concentrated around the high tide (HT) line, and the remaining 2.1 % were collected from the backshore (BS) area. However, none was found in the low tide line. Besides the sites S3 and S9, the average abundance of MPs on beaches was 247.6 ± 125.6 items/m^2. The average number in HT and BS areas was 486.7 ± 243.1 items/m^2 and 10.3 ± 8.7 items/m^2, respectively. In HT zones, the maximum abundance of MPs was 1476.0 ± 644.4 items/m^2 at S2 HT, and the minimum abundance was 88.6 ± 40.2 items/m^2 at S4 HT. In BS zones, MPs were only detected in two sites, with an average value of 52.2 ± 52.0 items/m^2 in S2 BS and 16.2 ± 4.8 items/m^2 in S8 BS, respectively. A detailed overview of MPs collected on the beaches of Yantai is provided in Table 1.

The investigation of MPs abundance in beach sediments has already been conducted worldwide (Table 2). By comparison of the studies using similar sampling and processing methods, the abundance of MPs from this event was at the same level as those on beaches of South Carolina, Dubai, and Brazil (Gray et al., 2018; Aslam et al., 2020; Maynard et al., 2021). The MPs abundances observed on beaches of Taiwan, Tenerife and Auckland were about twice as many as our results, but still as same order of magnitude (Kunz et al., 2016; Alvarez-Hernandez et al., 2019; Bridson et al., 2020). Considering that the background MPs pollution has been removed from the sampling results, the MP's abundance on the beaches of Yantai has been raised to a considerable level.

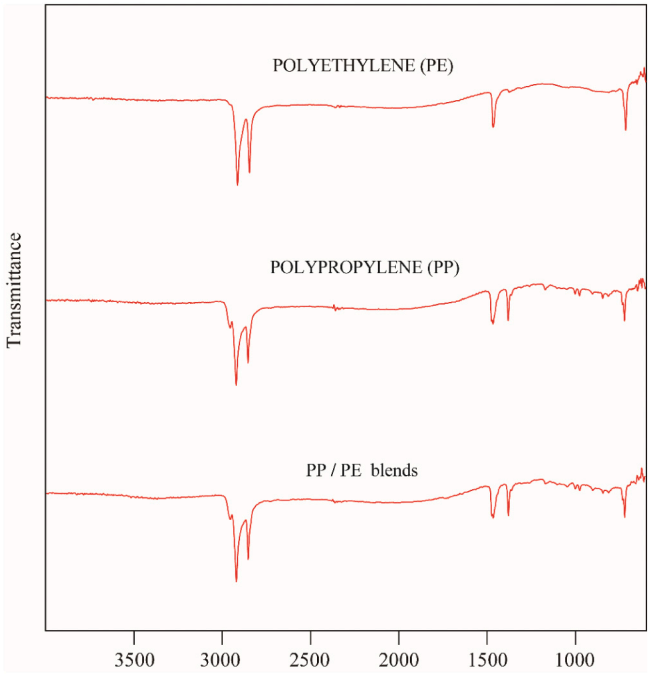

Fig. 2. FT-IR spectra of MPs in the sediments from beaches of Yantai.

3.2. Size and composition characteristics of MPs

Ellipsoid was the most frequently observed shape and accounted for 95.1 % of all identified MPs, while only 4.9 % were cylinder. Meanwhile, >99.9 % of MPs remained the original shape without obvious fracture due to timely sampling after reaching the beach. At the same time, only 4 plastic particles were broken or damaged into smaller and irregularly shaped particles and removed from the statistics of morphology features.

The average length of all MPs was 4.10 ± 0.31 cm (size range: 2.74 to 4.62 cm). The average length of the major and minor axis of ellipsoidal MPs were 4.23 ± 0.29 cm (size range: 3.79 to 4.62 cm) and 3.86 ± 0.27 cm (size range: 2.99 to 3.62 cm), respectively. The average length of the height, the major and minor axis and of columnar MPs were 3.22 ± 0.29 cm (size range: 2.74 to 4.01 cm), 3.42 ± 0.09 cm (size range: 2.99 to 3.55 cm), and 2.92 ± 0.22 cm (size range: 2.56 to 3.30 cm) respectively.

Three different polymer types were identified in selected MPs samples (Fig. 2), including polyethylene (70 %, PE), polypropylene (12 %, PP), and PP/PE blends (18 %). The results of the polymer types indicated that the MPs on beaches in Yantai came from leakage of PE and PP masterbatches. Meantime, varied types of polymers were detected in the sediment of different beaches in previous studies, such as rayon from clothes, polypropylene, polystyrene, polyvinyl chloride from packing bags or boxes, polypropylene and polyamide from fishing tools, polyphenylene sulfide from ships (Gao et al., 2021; Dowarah and Devipriya, 2019).

3.3. Weight and volume of MPs

The dry weight of MPs ranged from 0.44 ± 0.13 g/m^2 (S8 BS) to 50.78 ± 22.17 g/m^2 (S2 HT). Moreover, the mean weight of individual particles ranged from 0.0233 ± 0.0024 g/items (S5 HT) to 0.0376 ± 0.0036 (S7 HT) (Table 3). The average weight of individual ellipsoidal and columnar MPs was 0.0344 g/items and 0.0239 g/items, respectively. The ellipsoidal MPs were 30.5 % heavier than the columnar ones. There were no significant differences in the size and weight of MPs among different sites ($P > 0.05$). Based on Eqs. (2-1) and (2-2), the average ellipsoidal and columnar MPs volume was 36.12 cm^3 and

Table 3
The weight of MPs with different shapes in beach sediments collected from different sites.

	S1 HT	S2 HT	S2 BS	S4 TH	S5 HT	S6 HT	S7 HT	S8 HT	S8 BS
Weight of ellipsoidal MPs (g/m^2)	29.43 ± 17.93	50.78 ± 22.17	1.92 ± 1.91	3.08 ± 1.40	8.73 ± 4.31	6.05 ± 4.36	3.62 ± 2.42	10.35 ± 3.28	0.44 ± 0.13
Weight of columnar MPs (g/m^2)	0.20 ± 0.19	2.71 ± 1.17	0.10 ± 0.10	–	0.48 ± 0.28	0.30 ± 0.27	0.21 ± 0.20	0.10 ± 0.11	–
Average weight of each ellipsoidal MP (g/items)	0.0350 ± 0.0036	0.0344 ± 0.0040	0.0367 ± 0.0049	0.0348 ± 0.0033	0.0335 ± 0.0032	0.0350 ± 0.0036	0.0376 ± 0.0036	0.0340 ± 0.0034	0.0272 ± 0.0029
Average weight of each columnar MP (g/items)	0.0238 ± 0.0022	0.0240 ± 0.0023	0.0244 ± 0.0024	–	0.0233 ± 0.0024	0.0239 ± 0.0023	0.0240 ± 0.0023	0.0248 ± 0.0025	–

25.13 cm^3. The volume of ellipsoidal MPs was 30.6 % larger than the columnar. Based on Eqs. (2-3) to (2-7), the total quantity, weight, and volume of MPs in contaminated beaches were estimated to be 1.50×10^7 items, 514.67 kg and 536.33 m^3. The inventory of MPs in various marine habitats varied enormously in previous studies. The total quantity of MPs in Yugang Park beach (Zhanjiang Province) was estimated to be 1.18×10^5 items in winter and 2.95×10^5 items in summer (Zhang et al., 2020). The inventory of MPs was calculated as 1.20×10^{13} items (183.73 tons) in Sanggou Bay, China (Sui et al., 2020). The storage of MPs was 37 tons in surface sediments and 185 tons in deep sediments (−5 to −60 cm) of Beibu Gulf, China (Xue et al., 2020). Moreover, the MPs inventory was referred to be 700 tons in the surface seawater of the entire South China Sea (Cai et al., 2018). Considering that the inventory of MPs in terrestrial and aquatic environment came from years of accumulation, total input of MPs from this leakage was two orders of magnitude higher than the inventory in the Yugang Park beach and two or more orders of magnitude lower than the inventory in the seawater or sediments of China's coastal regions. Thus, its influence on the overall environment of the Bohai Sea might be unneglectable. Moreover, since the considerable level of MPs pollution on beaches of Yantai has been raised by this event alone, the potential effect of MPs leakage on the Yantai coastal area might be sustained and serious, and further research might be needed.

3.4. Wind and ocean circulation

From November 17, 2020, to January 16, 2021, the transmission areas of MPs in the Bohai Sea area were dominated by northerly wind (>81.7 %) with an average wind speed of 15.8 km/h and an average horizontal angle of 320.26° (Figs. 4 and 5). Meantime, in December 2020, the direction distribution of wind in the Bohai Sea was more discrete between north and west with northerly wind speed of 16.3 km/h. On January 1–16, 2021, the direction distribution of wind was more concentrated in northwest than in December 2020, with an average northerly wind speed of 14.8 km/h.

The hydrodynamic modeling results show that the surface current of the Bohai Sea was mainly wind-induced current and the southern current accounted for >89.2 %. The water entered the Bohai Sea through the north of the Bohai strait and left from the south of the strait. Yantai was located at the southern end of the Bohai strait and was mainly affected by the southeast current. The simulation result of the Bohai circulation was highly consistent with former studies (Li et al., 2018; Cao and Lou, 2011).

3.5. The transports and source of MPs

When the wind drag is activated in Scenario 1 (Fig. 6), the MPs moved northwestward along the coastline, steered to the east and then north, and reached east-central the Bohai Strait on 5th simulation day. And then >96 % of MPs traveled northwestward through the Bohai Strait and Bohai Sea, and reached Tangshan Port in Hebei Province (118.7°E, 39.1°N) in 18.4 simulation days. The MPs traveled over 365.70 km at an average speed of about 21.51 km/day from December 30 to January 16. Since then, the MPs were gathered along the north coastal area of BHB and trapped nearby this area until the end of the simulation. Meanwhile, the speed of the movement was reduced to 6.70 km/day (Fig. 6). In Scenario 2 (Fig. 6B), the MPs moved 147.18 km from the release zone to the middle of the Bohai Strait (120.6°E, 38.4°N) on December 30 with an average speed of about 8.66 km/day. About 66 % of MPs remained in oscillatory motion nearby this region through the simulating experiment. In comparison, 34 % of MPs crossed the Bohai Strait and arrived at the middle of the Bohai Sea on the 60th simulation day. Therefore, the oscillation induced by the tidal current significantly reduced MP's transmission speed and travel distance, revealing the crucial role of tide action in transporting MPs. Under the influence of wind drag on the sea surface (Scenario 1), the horizontal

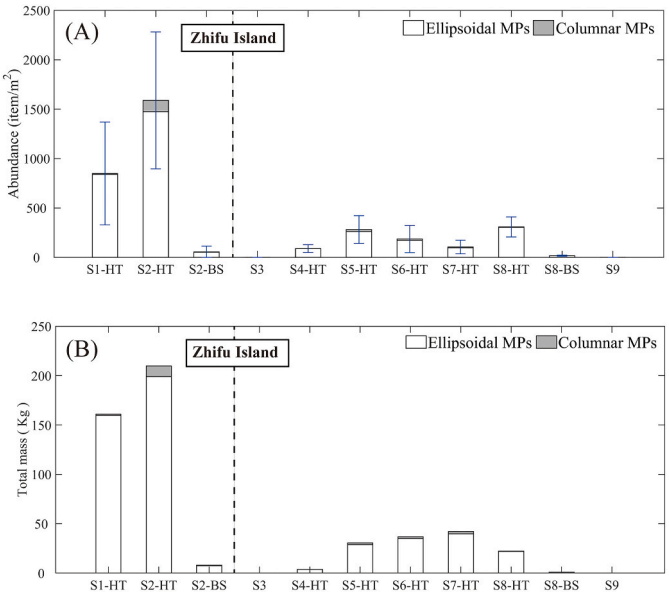

Fig. 3. Abundance (A) and estimated total mass (B) of MPs in beach sediments of Yantai. The 9 sampling sites were divided into west part (S1 and S2) and east part (S3-S9) by the Zhifu Island.

moving range of MPs was 59.75 % larger than that in Scenario 2. Moreover, when the northward wind cooperated with the eastward current from 2020 to early 2021, it only took <19 days for MPs to cross the Bohai Sea and travel from Tangshan Port to Yantai. Previous studies also revealed that wind drift might significantly change the distribution of MPs along the coastline and promote long-distance transmission of MPs (Tsiaras et al., 2021; Alosairi et al., 2020).

The simulation trajectory in Scenario 1 (Fig. 6A) indicated that two days (January 15–16) before the arrival on the beach of Yantai, under the influence of northwest wind and eastward coastal current, MPs were moving along the coastline from west to east, which might induce a part of moving eastward MPs blocked by Zhifu Island and accumulated in the west of Zhifu Island (in S1 and S2). In addition, the survey results validated that the abundance and weight of MPs in the western sites (S1 and S2) of Zhifu Island were about 5 times as many as in the eastern sites (S4-S8), and no MPs were found in S3 (Fig. 3). Therefore, both simulation and survey data appear to confirm that the distribution of MPs in the coastal area is impacted not only by the dynamic conditions (wind, tide, and current) but also by the geometry of coastline (Zhang, 2017).

Since the direction of wind and current in the backward simulation was contrary to those in the actual situation, the leaked MPs followed the same trajectory but moved in the opposite direction and from the destination to the source. Due to the absence of direct evidence, the results of backward simulation only indicated the possible source of MPs and the transmission path. Thus, any location along the moving track could be the leaking point (Fig. 6).

4. Conclusion

Our research suggested that the MPs came from leakage of polyethylene and polypropylene masterbatches with a total input of 1.50×10^7 items (514.67 kg). The incident affected 7 beaches and 32.8 km of coastline with an MPs abundance of 247.6 ± 125.6 items/m^2

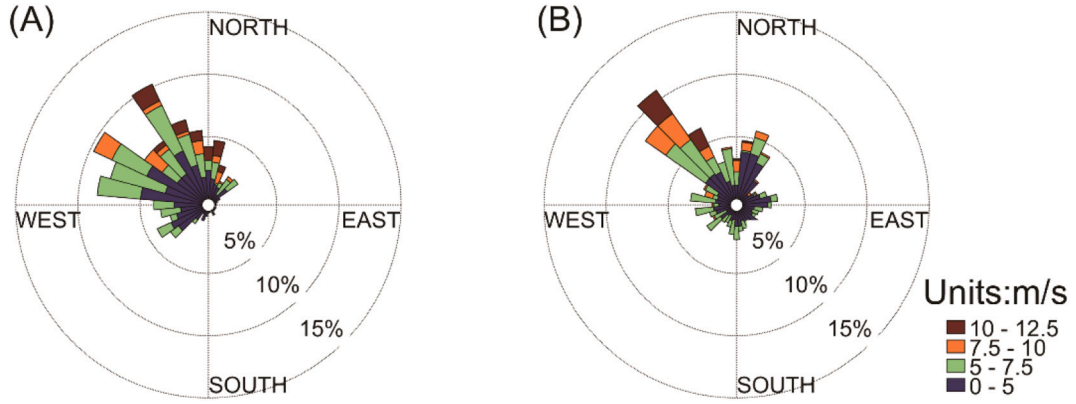

Fig. 4. Wind rose based on the ECMWF data during December 2020 (A) and in January 1–16, 2021 (B) in Bohai Sea.

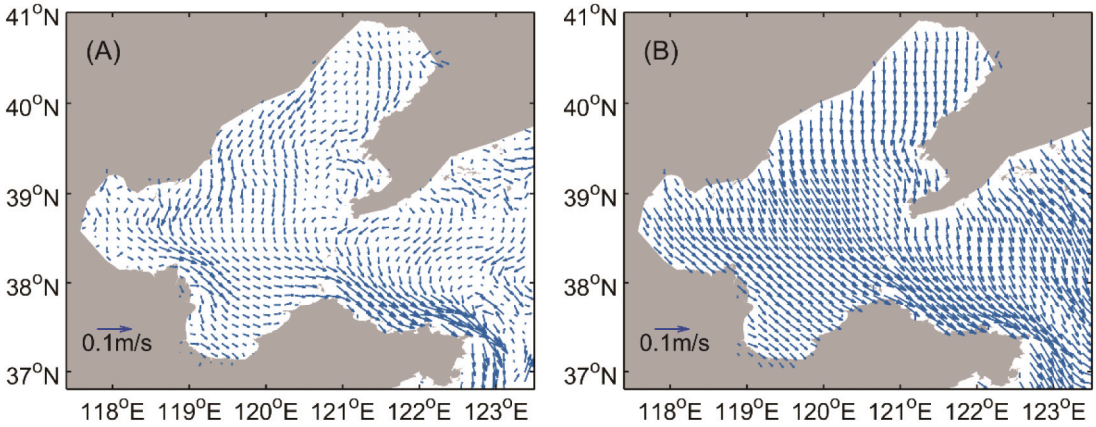

Fig. 5. The simulation results of time-average surface current (A) and combination of current and wind drag on the sea surface (B) during simulation.

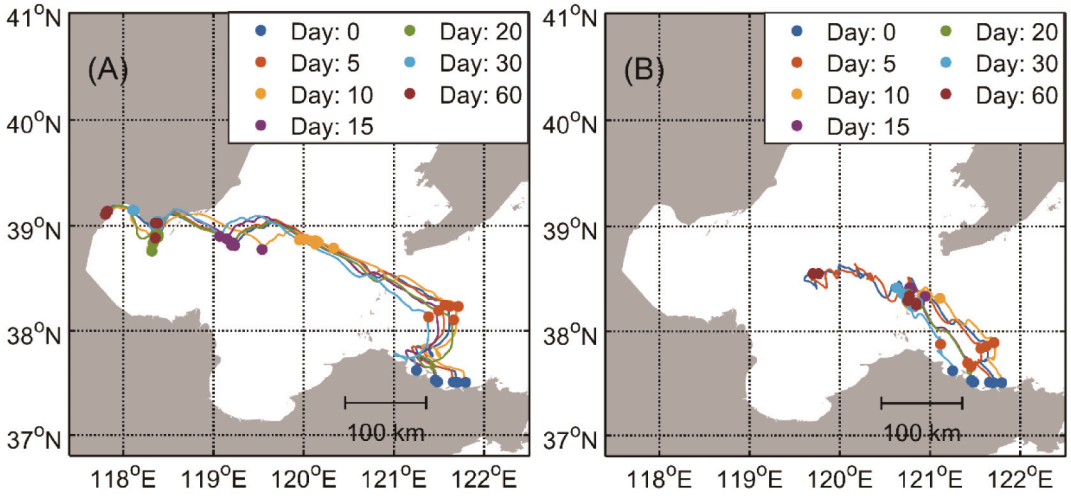

Fig. 6. The simulation results of MPs source tracking with (A) and without (B) wind drag on sea surface. Lines of different colors stand for the trajectories of MPs from different sampling sites. Dots of different colors stand for arrival locations of MPs at different simulation time.

in contaminated beaches. Driven by northwest wind and wind-induced surface current, the MPs traveled over 360 km, crossed the Bohai Sea and arrived at the coast of Yantai in <18 days. However, due to lack of direct proof, the simulation results might only indicate the range of leaking sources, which was moving track of MPs. In addition, our results confirmed that an irregular coastline might obviously alter the distribution of MPs in beach sediment, and the numerical model was a useful tool to reveal the transport process of MPs in the coastal environments.

CRediT authorship contribution statement

Chen Zhang: Investigation, Data curation, Formal analysis, Visualization, Validation, Writing – original draft, Writing – review & editing. **Qing Wang:** Conceptualization, Resources, Validation, Writing – original draft, Writing – review & editing, Supervision, Project administration, Funding acquisition. **Jianmin Zhao:** Conceptualization, Resources, Methodology, Writing – review & editing, Funding acquisition. **Yingjie Zhao:** Investigation, Data curation, Formal analysis. **Encui Shan:** Investigation, Data curation, Writing – review & editing.

Declaration of competing interest

The authors declare that they have no known competing financial interests or personal relationships that could have appeared to influence the work reported in this paper.

Data availability

Data will be made available on request.

Acknowledgements

This study was supported by the Strategic Priority Research Program of the Chinese Academy of Sciences (XDA23050303), the National Natural Science Foundation of China (42176161), the National Key Research and Development Program (2019YFD0901101) and the Two-Hundred Talents Plan of Yantai (Y839081021).

Appendix A. Supplementary data

Supplementary data to this article can be found online at https://doi.org/10.1016/j.marpolbul.2022.113976.

References

Alosairi, Y., Al-Salem, S.M., Ragum, A.A., 2020. Three-dimensional numerical modelling of transport, fate and distribution of microplastics in the northwestern Arabian/Persian Gulf[J]. Mar. Pollut. Bull. 161 (Pt B), 111723.
Alvarez-Hernandez, C., Cairos, C., Lopez-Darias, J., Mazzetti, E., Hernandez-Sanchez, C., Gonzalez-Salamo, J., Hernandez-Borges, J., 2019. Microplastic debris in beaches of Tenerife (Canary Islands, Spain). Mar. Pollut. Bull. 146, 26–32.
Aslam, H., Ali, T., Mortula, M.M., Attaelmanan, A.G., 2020. Evaluation of microplastics in beach sediments along the coast of Dubai, UAE. Mar. Pollut. Bull. 150, 110739.
Besseling, E., Quik, J., Sun, M., Koelmans, A., 2016. Fate of nano- and microplastic in freshwater systems: a modeling study. Environ. Pollut. 220.
Brickman, D., Smith, P., 2002. Lagrangian stochastic modeling in coastal oceanography. J. Atmos. Ocean. Technol. 19, 83–99.
Bridson, J.H., Patel, M., Lewis, A., Gaw, S., Parker, K., 2020. Microplastic contamination in Auckland (New Zealand) beach sediments. Mar. Pollut. Bull. 151, 110867.
Cai, M., He, H., Liu, M., et al., 2018. Lost but can't be neglected: huge quantities of small microplastics hide in the South China Sea. Sci. Total Environ. 633, 1206–1216.
Cao, Z., Lou, A., 2011. A Three Dimensional Numerical Simulation of the Wind-Driven Circulation During December in the Bohai Sea by FVCOM. Periodical of Ocean University of China.
Constant, M., Ludwig, W., Kerherve, P., Sola, J., Charriere, B., Sanchez-Vidal, A., Canals, M., Heussner, S., 2020. Microplastic fluxes in a large and a small Mediterranean river catchments: the Tet and the Rhone, Northwestern Mediterranean Sea. Sci. Total Environ. 716, 13.
Ding, Y., et al., 2019. Observational and model studies of synoptic current fluctuations in the Bohai Strait on the chinese continental shelf. Ocean Dyn. 69 (3), 323–351.
Dowarah, K., Devipriya, S.P., 2019. Microplastic prevalence in the beaches of Puducherry, India and its correlation with fishing and tourism/recreational activities. Mar. Pollut. Bull. 148, 123–133.
Eriksen, M., Lebreton, L., Carson, H., Thiel, M., Moore, C., Borerro, J., Galgani, F., Ryan, P., Reisser, J., 2014. Plastic pollution in the World's Oceans: more than 5 trillion plastic pieces weighing over 250,000 tons afloat at Sea. PLoS ONE 9.
Frère, L., Paul-Pont, I., Rinnert, E., Petton, S., Jaffré, J., Bihannic, I., Soudant, P., Lambert, C., Huvet, A., 2017. Influence of environmental and anthropogenic factors on the composition, concentration and spatial distribution of microplastics: a case study of the bay of Brest (Brittany, France). Environ. Pollut. 225, 211–222.
Gao, F., Li, J., Hu, J., Sui, B., Wang, C., Sun, C., Li, X., Ju, P., 2021. The seasonal distribution characteristics of microplastics on bathing beaches along the coast of Qingdao, China. Sci. Total Environ. 783, 146969.
Genc, A.N., Vural, N., Balas, L., 2020. Modeling transport of microplastics in enclosed coastal waters: a case study in the Fethiye Inner Bay. Mar. Pollut. Bull. 150, 110747.
Goodwin, J., Munroe, D., Defne, Z., Ganju, N., Vasslides, J., 2019. Estimating connectivity of hard clam (Mercenaria mercenaria) and eastern oyster (Crassostrea virginica) larvae in Barnegat Bay. J. Mar. Sci. Eng. 7 (167), 17.
Gray, A.D., Wertz, H., Leads, R.R., Weinstein, J.E., 2018. Microplastic in two South Carolina estuaries: occurrence, distribution, and composition. Mar. Pollut. Bull. 128, 223–233.
Hardesty, B.D., Harari, J., Isobe, A., et al., 2017. Using numerical model simulations to improve the understanding of micro-plastic distribution and pathways in the marine environment. Front. Mar. Sci. 4, 30.
Jambeck, J., Geyer, R., Wilcox, C., Siegler, T., Perryman, M., Andrady, A., Narayan, R., Law, K., 2015. Marine pollution. Plastic waste inputs from land into the ocean. Science 347, 768–771.
Jiang, Y., Yang, F., Zhao, Y.A., Wang, J., 2020. Greenland Sea gyre increases microplastic pollution in the surface waters of the nordic seas. Sci. Total Environ. 712, 9.

Kunz, A., Walther, B.A., Löwemark, L., Lee, Y.-C., 2016. Distribution and quantity of microplastic on sandy beaches along the northern coast of Taiwan. Mar. Pollut. Bull. 111, 126–135.
Lee, J., Lee, J.S., Jang, Y.C., Hong, S.Y., Shim, W.J., Song, Y.K., Hong, S.H., Jang, M., Han, G.M., Kang, D., Hong, S., 2015. Distribution and size relationships of plastic marine debris on beaches in South Korea. Arch. Environ. Contam. Toxicol. 69, 288–298.
Lee, J., Lee, J., Hong, S., Hong, S.H., Shim, W.J., Eo, S., 2017. Characteristics of meso-sized plastic marine debris on 20 beaches in Korea. Mar. Pollut. Bull. 123, 92–96.
Li, M., Zhong, L., Boicourt, W., 2005. Simulations of Chesapeake Bay estuary: sensitivity to turbulence mixing parameterizations and comparison with observations. J. Geophys. Res. Oceans 110.
Li, R., Yu, L., Chai, M., Wu, H., Zhu, X., 2020. The distribution, characteristics and ecological risks of microplastics in the mangroves of southern China. Sci. Total Environ. 708, 135025.
Li, Y., Wolanski, E., Dai, Z., Lambrechts, J., Tang, C., Zhang, H., 2018. Trapping of plastics in semi-enclosed seas: insights from the Bohai Sea, China. Mar. Pollut. Bull. 137, 509–517.
Liubartseva, S., Coppini, G., Lecci, R., Creti, S., 2016. Regional approach to modeling the transport of floating plastic debris in the Adriatic Sea. Mar. Pollut. Bull. 103 (1–2), 115–127.
Maynard, I.F.N., et al., 2021. Analysis of the occurrence of microplastics in beach sand on the brazilian coast. Sci. Total Environ. 771, 144777.
Mo, D., Hou, Y., Li, J., Liu, Y., 2016. Study on the storm surges induced by cold waves in the northern East China Sea. J. Mar. Syst. 160.
Munari, C., et al., 2017. Microplastics in the sediments of Terra Nova Bay (Ross Sea, Antarctica). Mar. Pollut. Bull. 122 (1), 161–165.
Neumann, D., Callies, U., Matthies, M., 2014. Marine litter ensemble transport simulations in the southern North Sea. Mar. Pollut. Bull. 86.
North, E., Schlag, Z., Hood, R., Li, M., Zhong, L., Gross, T., Kennedy, V., 2008. Vertical swimming behavior influences the dispersal of simulated oyster larvae in a coupled particle-tracking and hydrodynamic model of Chesapeake Bay. Mar. Ecol. Prog. Ser. 359, 99–115.
Peng, L., Fu, D., Qi, H., Lan, C.Q., Yu, H., Ge, C., 2020. Micro- and nano-plastics in marine environment: source, distribution and threats - a review. Sci. Total Environ. 698, 134254.
Piñon-Colin, T.D.J., Rodriguez-Jimenez, R., Pastrana-Corral, M.A., Rogel-Hernandez, E., Wakida, F.T., 2018. Microplastics on sandy beaches of the Baja California Peninsula, Mexico. Mar. Pollut. Bull. 131, 63–71.
Plastics Europe, 2018. Plastics-the Facts 2018: An Analysis of European Plastics Production, Demand and Waste Data for 2017.
Pohl, F., Eggenhuisen, J.T., Kane, I.A., Clare, M.A., 2020. Transport and burial of microplastics in deep-marine sediments by turbidity currents. Environ. Sci. Technol. 54 (7), 4180–4189.
Qiu, Q., Tan, Z., Wang, J., Peng, J., Li, M., Zhan, Z., 2016. Extraction, enumeration and identification methods for monitoring microplastics in the environment. Estuar. Coast. Shelf Sci. 176, 102–109.
Rochman, C., 2018. Microplastics research—from sink to source. Science 360, 28–29.
Shchepetkin, A., McWilliams, J., 2005. The regional oceanic modeling system (ROMS): a split-explicit, free-surface, topograph-following- coordinate ocean model. Ocean Model. 9, 347–404.
Sherman, P., van Sebille, E., 2016. Modeling marine surface microplastic transport to assess optimal removal locations. Environ. Res. Lett. 11 (1).
Su, L., Xiong, X., Zhang, Y., Wu, C., Xu, X., Sun, C., Shi, H., 2022. Global transportation of plastics and microplastics: a critical review of pathways and influences. Sci. Total Environ. 831, 154884.
Sui, Q., Zhang, L., Xia, B., et al., 2020. Spatiotemporal distribution, source identification and inventory of microplastics in surface sediments from Sanggou Bay, China. Sci. Total Environ. 723, 138064.
Teng, J., Zhao, J.M., Zhang, C., Cheng, B., Koelmans, A.A., Wu, D., Gao, M., Sun, X.Y., Liu, Y.L., Wang, Q., 2020. A systems analysis of microplastic pollution in Laizhou Bay, China. Sci. Total Environ. 745.
Teng, J., Zhao, J.M., Zhu, X.P., Shan, E.C., Zhang, C., Zhang, W.J., Wang, Q., 2021. Toxic effects of exposure to microplastics with environmentally relevant shapes and concentrations: accumulation, energy metabolism and tissue damage in oyster Crassostrea gigas. Environ. Pollut. 269.
Thompson, R., Olsen, Y., Mitchell, R., Davis, A., Rowland, S., John, A., McGonigle, D.F., Russell, A., 2004. Lost at sea: where is all the plastic? Science 304, 838.
Tsiaras, K., Hatzonikolakis, Y., Kalaroni, S., Pollani, A., Triantafyllou, G., 2021. Modeling the pathways and accumulation patterns of micro- and macro-plastics in the Mediterranean. Front. Mar. Sci. 8.
Wang, J., Li, Y., Lu, L., Zheng, M., Zhang, X., Tian, H., Wang, W., Ru, S., 2019. Polystyrene microplastics cause tissue damages, sex-specific reproductive disruption and transgenerational effects in marine medaka (Oryzias melastigma). Environ. Pollut. 254, 113024.
Xue, B., Zhang, L., Li, R., et al., 2020. Underestimated microplastic pollution derived from fishery activities and “hidden” in deep sediment. Environ. Sci. Technol. 54 (4), 2210–2217.
Zhang, B., Wu, D., Yang, X., Teng, J., Liu, Y.L., Zhang, C., Zhao, J.M., Yin, X.N., You, L.P., Liu, Y.F., Wang, Q., 2019. Microplastic pollution in the surface sediments collected from Sishili Bay, North Yellow Sea, China. Mar. Pollut. Bull. 141, 9–15.
Zhang, H., 2017. Transport of microplastics in coastal seas. Estuar. Coast. Shelf Sci. 199, 74–86.
Zhang, X., Munroe, D., Haidvogel, D., Powell, E., 2016. Atlantic surfclam connectivity within the Middle Atlantic Bight: mechanisms underlying variation in larval transport and settlement. Estuar. Coast. Shelf Sci. 173.
Zhang, Z., Wu, H., Peng, G., Xu, P., Li, D., 2020. Coastal Ocean dynamics reduce the export of microplastics to the open ocean. Sci. Total Environ. 713, 136634.
Zhao, J., Ran, W., Teng, J., Liu, Y., Cao, R., Wang, Q., Yin, X., 2018. Microplastic pollution in sediments from the Bohai Sea and the Yellow Sea, China. Sci. Total Environ. 640, 637–645.